Calibration in Multiconductor Transmission Lines

Dylan F. Williams, *Senior Member, IEEE*

National Institute of Standards and Technology

***Abstract*- This paper presents a calibration and measurement method for circuits embedded in lossy printed multiconductor transmission lines. The experimental results illustrate the complexity of the modal representation and the utility of the conductor representation for circuit design.**

INTRODUCTION

This paper presents a method based on the procedure of [1] for measuring the impedance matrices of one-port circuits embedded in multiconductor transmission lines. The method determines both the modal and the "power-normalized" conductor impedance matrices of [2] and [3] describing the embedded device. We use a simple resistive circuit embedded in a pair of lossy asymmetric coupled microstrip lines to illustrate the method.

We use the procedure of [1] to characterize the multiconductor transmission line in which the device is embedded. That procedure applies the weighted orthogonal distance regression algorithm of [4] to find the matrices of transmission line impedances and admittances per unit length that best reproduce a number of two-port scattering-parameter measurements performed on multiple lengths of a multiconductor transmission line. The procedure of [1] can determine all of the conductor parameters of the line without making any assumptions: this verifies that the line's conductor impedance matrix $\underline{G}_c$ is small, its conductor capacitance matrix $\underline{C}_c$ is symmetric and nearly frequency

Reprinted from 48th ARFTG Conf. Digest, pp. 46-53, Fall 1996.

independent, and its resistance and inductance matrices $\underline{R}_c$ and $\underline{L}_c$ are symmetric, assumptions that we checked with the full-wave calculation method of [5].

Accuracy is improved by setting $\underline{G}_c$ to 0 and all of the other matrices symmetric, which reduces the number of variables that must be determined by the algorithm. We repeated the optimization with these assumptions to determine the low-frequency limit of $\underline{C}_c$ and then with $\underline{C}_c$ set to this low-frequency limit to determine $\underline{R}_c$ and $\underline{L}_c$. At this final stage of the analysis we can also add a reciprocal error box to the model to account for transition parasitics.

In this work we use the electrical model of the multiconductor transmission line determined by this procedure to de-embed the electrical parameters of circuits embedded in the line. Since the method of [1] determines both modal and conductor representations for the line, we are able to determine both the modal and conductor impedance matrices describing the embedded device.

MODAL REPRESENTATION

The total transverse electric field $\boldsymbol{E}_t$ and magnetic field $\boldsymbol{H}_t$ in a closed transmission line that is uniform in z and constructed of linear isotropic materials can be written as [6]

$$\boldsymbol{E}_t = \sum_n \frac{v_{mn}(z)}{v_{0n}}\, \boldsymbol{e}_{tn} \ ; \quad \boldsymbol{H}_t = \sum_n \frac{i_{mn}(z)}{i_{0n}}\, \boldsymbol{h}_{tn}, \tag{1}$$

where v_{mn} and i_{mn} are the modal voltages and currents of the nth mode, $\boldsymbol{e}_{tn}$ and $\boldsymbol{h}_{tn}$ are its transverse modal electric and magnetic fields (functions only of the transverse coordinates x and y), the sums span all of the excited modes in the line, and the time-harmonic dependence $e^{+j\omega t}$, where ω is the real angular frequency, has been suppressed. In open guides we must add a continuous spectrum of modes to this discrete set [7], which we assume that we can neglect.

We restrict the normalizing voltages v_{0n} and currents i_{0n} by $v_{0n}\, i_{0n}^* \;=\; p_{0n} \equiv \int_S \boldsymbol{e}_{tn} \times \boldsymbol{h}_{tn}^* \cdot \boldsymbol{z}\, \mathrm{d}S$, where $\mathrm{Re}(p_{0n}) \geq 0$ so that the complex power carried in the forward direction by the nth forward and backward modes in the absence of any other modes in the guide is given by $v_{mn}\, i_{nm}^*$. This is the conventional normalization and corresponds to the power condition used in [1], [2], and [8] and suggested by Brews [9]. The characteristic impedance of the nth mode is $Z_{0n} \equiv v_{0n}/i_{0n} = |v_{0n}|^2/p_{0n}^* = p_{0n}/|i_{0n}|^2$; its magnitude is fixed by the choice of $|v_{0n}|$ or $|i_{0n}|$ while its phase is fixed by p_{0n}.

When a finite number of discrete modes are excited in the line, the total complex power p carried in the forward direction is

$$p = \int \boldsymbol{E}_t \times \boldsymbol{H}_t^* \cdot \boldsymbol{z}\, \mathrm{d}S = \sum_{n,k} \frac{v_{mn}}{v_{0n}} \frac{i_{mk}^*}{i_{0k}^*} \int \boldsymbol{e}_{tn} \times \boldsymbol{h}_{tk}^* \cdot \boldsymbol{z}\, \mathrm{d}S = \underline{i}_m^\dagger \underline{X}\, \underline{v}_m, \qquad \textbf{(2)}$$

where the superscript † indicates the Hermitian adjoint (conjugate transpose), the elements of the cross-power matrix $\underline{X}$ are defined by $X_{nk} \equiv (v_{0k} i_{0n}^*)^{-1} \int \boldsymbol{e}_{tk} \times \boldsymbol{h}_{tn}^* \cdot \boldsymbol{z}\ \mathrm{d}S$, $X_{nn} = 1$, and the integrals are performed over the entire transmission-line cross section [1]. Choosing $v_{0n} = -\int_{\text{path}} \boldsymbol{e}_{tn} \cdot \mathrm{d}l$ ensures that $v_n = -\int_{\text{path}} \boldsymbol{E}_t \cdot \mathrm{d}l$ when only the nth forward and backward modes are excited in the line [8]. Likewise choosing $i_{0n} = \oint_{\text{path}} \boldsymbol{h}_{tn} \cdot \mathrm{d}l$ ensures that $i_n = \oint_{\text{path}} \boldsymbol{h}_t \cdot \mathrm{d}l$. The modal impedance matrix $\underline{Z}_m$ of a linear one-port device embedded in the line relates $\underline{v}_m$ and $\underline{i}_m$ by $\underline{v}_m = \underline{Z}_m\, \underline{i}_m$.

To illustrate the behavior of the modal impedance matrix we applied the procedure of [1] to two asymmetric coupled microstrip lines with widths of 54 µm and 254 µm separated by a gap of 45 µm printed on an alumina substrate with an approximate thickness of 254 µm. The conductor metalization had a measured thickness of 1.8 µm and measured dc conductivity of $3.3\text{x}10^7\ \Omega^{-1}\cdot\text{m}^{-1}$. We used the transmission line model to de-embed the modal impedance matrix of two small planar resistors connected between the two conductors of the line and the ground plane on the back of the substrate with via holes from measurements of the circuit embedded in the coupled microstrip lines. As in [1] we defined the voltage path for the c mode, which corresponds to the even mode of a symmetric microstrip line, to be between the 254 µm wide microstrip conductor and the ground plane on the back of the substrate; we defined the voltage path for the π mode, which corresponds to the odd mode of a symmetric microstrip line, to be between the 254 µm and 54 µm wide microstrip conductors.

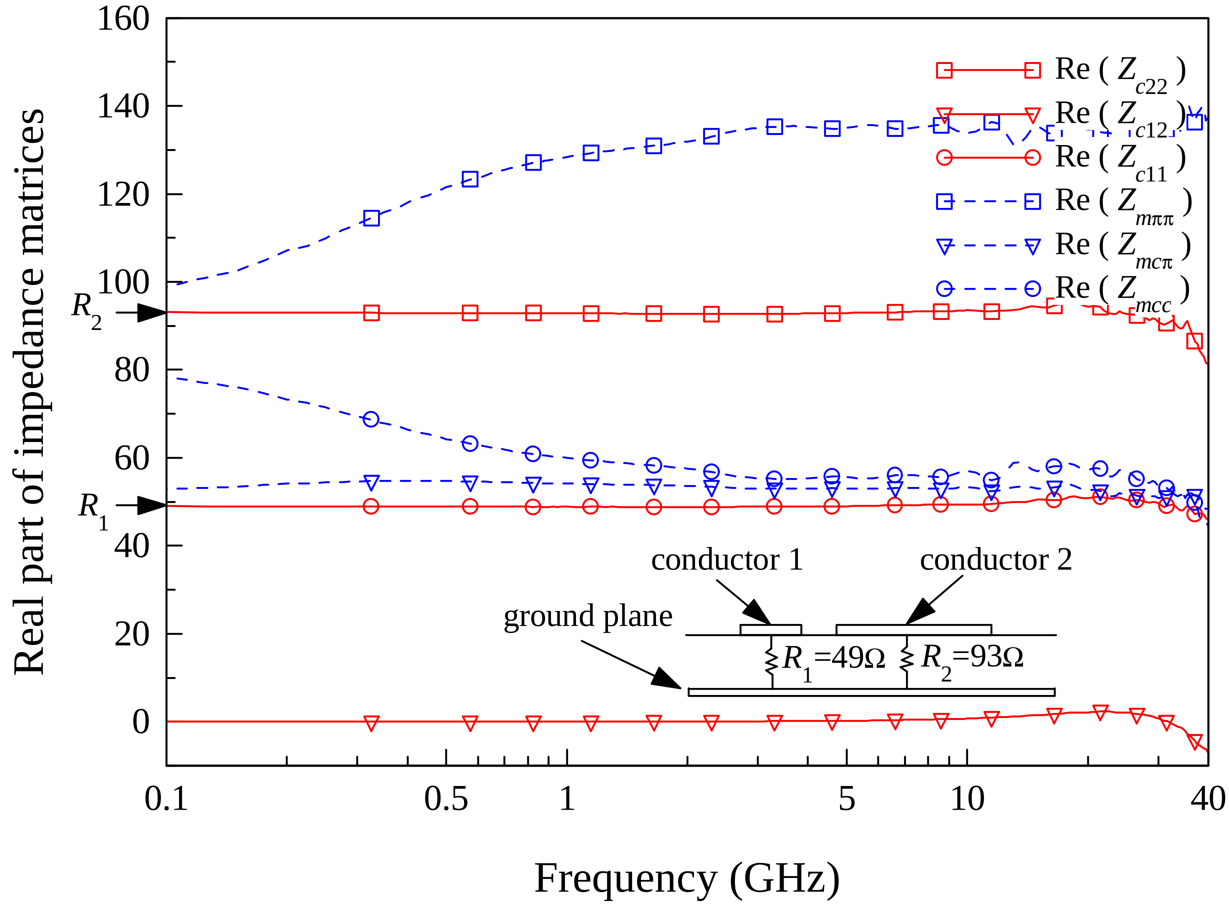

Figure 1. The real part of the elements of the modal impedance matrix $\underline{Z}_m$ and the conductor impedance matrix $\underline{Z}_c$ for two small resistors connected between the two conductors of a pair of asymmetric microstrip lines and the ground plane on the back of the substrate. The connections of the resistors are sketched in the lower right of the figure.

Figure 1 plots in dashed lines the real parts of the elements of the modal impedance matrix of the small circuit. The figure shows that the elements of $\underline{Z}_m$ are highly frequency dependent. This illustrates a serious drawback of the modal impedance matrix: its elements do not correspond to the impedances anticipated from simple physical models [10] despite the small size and lumped nature of the circuit. Circuit design in this modal representation is difficult not only because the impedance matrices do not correspond to anticipated circuit behavior, but also because the complex power is not equal to $\underline{i}_m^{\dagger}\,\underline{v}_m$.

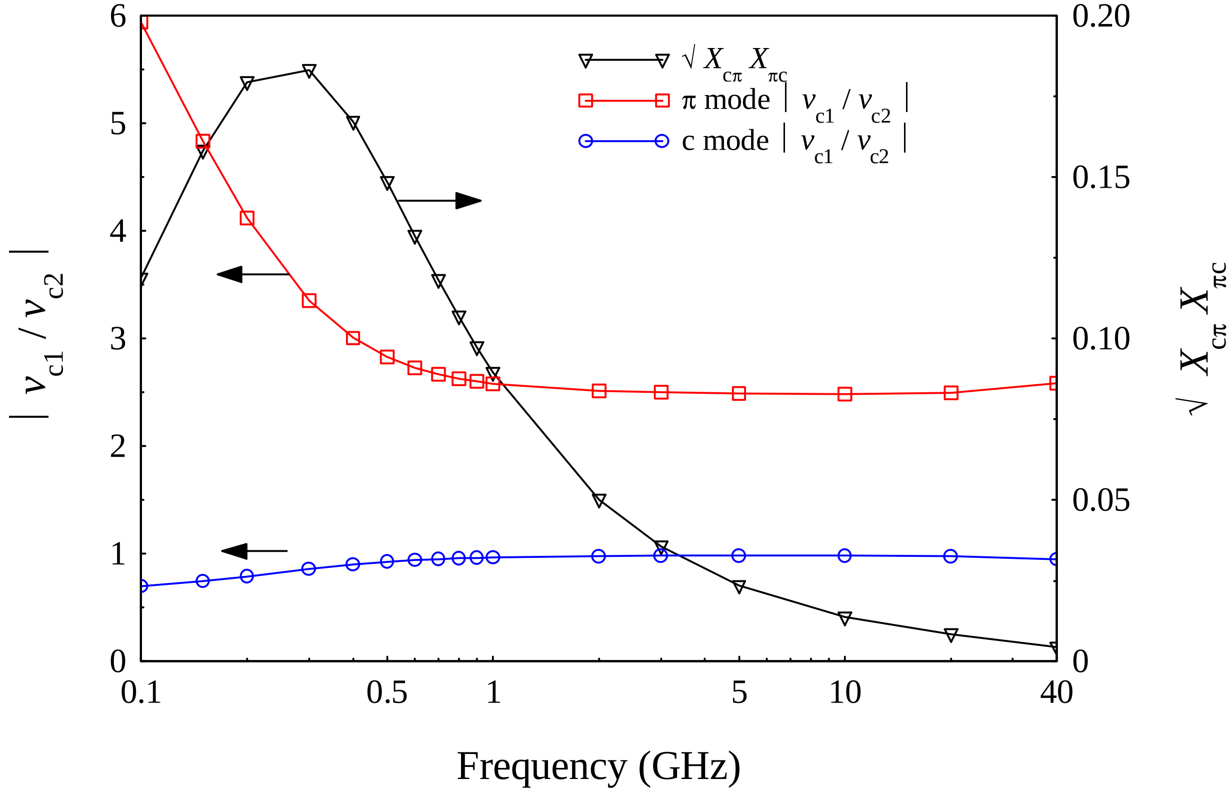

Figure 2. The magnitude of the ratios of the voltages impressed by the *c* and π modes between the 54 μm wide microstrip conductor and the ground (v_{c1}) and the 254 μm wide microstrip conductor and the ground (v_{c2}).

Figure 2 shows calculations of the ratio of the voltages impressed by the *c* and π modes between the two conductors and their grounds using the full-wave method of [5]; for the calculations we assumed that the substrate had a dielectric constant of 10 and was lossless. The figure shows that these ratios are not constant: they, and therefore the modal field configurations, change significantly near the peak in the off-diagonal elements of $\underline{X}$. This explains the frequency dependence of $\underline{Z}_m$, which reflects this complex modal behavior.

CONDUCTOR REPRESENTATION

Every excited mode in a multiconductor transmission line impresses a voltage across each of its conductors, so the total voltage between any given pair of its conductors is a linear combination of all of the modal voltages of the excited modes. Likewise the total current in any given conductor will be a linear combination of the modal currents. References [2] and [3] refer to these linear combinations of modal voltages and currents as the “conductor” voltages and currents.

The vectors of conductor voltages $\underline{v}_c$ and currents $\underline{i}_c$ of [2] and [3] are defined by $\underline{v}_c \equiv \underline{M}_v \, \underline{v}_m$ and $\underline{i}_c \equiv \underline{M}_i \, \underline{i}_m$, where $\underline{M}_v$ and $\underline{M}_i$ are unitless. The vectors $\underline{v}_c$ and $\underline{i}_c$ are “power-normalized” in [2] and [3] so that $p = \underline{i}_c^{\dagger} \, \underline{v}_c$: this requires that $\underline{M}_v$ and $\underline{M}_i$ satisfy $\underline{M}_i^{\dagger} \underline{M}_v = \underline{X}$. The conductor impedance matrix $\underline{Z}_c$ of a one-port device embedded in a line relates $\underline{v}_c$ and $\underline{i}_c$ by $\underline{v}_c = \underline{Z}_c \, \underline{i}_c$.

As in [1] we defined the voltage paths for $\underline{v}_{c1}$ and $\underline{v}_{c2}$ to be between the 54 µm and the 254 µm wide microstrip conductors, respectively, and the ground plane; these paths also correspond to the connection paths of our two resistors. Figure 1 plots the real parts of the elements of the conductor impedance matrix $\underline{Z}_c$ of the circuit in solid lines for this choice of paths. The figure shows that the real parts of the elements of $\underline{Z}_c$ are nearly constant with frequency and correspond closely to the measured dc resistances of the two small resistors, as we would expect from simple physical considerations [10]. We found that the imaginary parts of the elements of $\underline{Z}_c$ increased linearly from 0 with frequency and again correspond to behavior we would anticipate from physical considerations. In addition, since $\underline{v}_c$ and $\underline{i}_c$ are power normalized, the conductor impedance matrices can be used directly in conventional circuit simulators to predict circuit response and power flow [2].

CONCLUSION

We presented a method for the measurement of one-port circuits embedded in lossy asymmetric printed multiconductor transmission lines. The method illustrates the complexity of the modal representation and the advantages of using the power-normalized conductor representations of [2] and [3] in circuit design. The method makes possible fully corrected calibrations and measurements in lossy multiconductor transmission lines.

The elements of $\underline{Z}_c$ do not correspond to the anticipated behavior of the circuit solely because the voltage paths used to define $\underline{v}_{c1}$ and $\underline{v}_{c2}$ correspond to those connecting the resistors, but also because $\underline{v}_c$ and $\underline{i}_c$ are power normalized so that $p = \underline{i}_c^{\dagger} \underline{v}_c$. This power normalization must account for the off-diagonal elements of $\underline{X}$, which become significant when the modal propagation constants approach each other [11], and requires complex frequency dependent matrices $\underline{M}_v$ and $\underline{M}_i$. This shows that theories that assume real frequency independent relations between these quantities will fail in lossy asymmetric coupled microstrip lines.

In the asymmetric microstrip lines studied here the power-normalized representation of [2] and [3] and the reciprocity-based representation of [12] are nearly identical [2]; our results cannot be used to show that either one of these representations is preferable. Although not demonstrated here, the calibration method is also applicable to transmission lines with more than three conductors.

ACKNOWLEDGMENTS

We appreciate the contributions of Stefaan Sercu and Luc Martens at the University of Ghent in Ghent, Belgium, who made possible the measurements reported here.

REFERENCES

[1] D. F. Williams, “Multiconductor transmission line characterization,” submitted to *IEEE Trans. Comp., Packag., and Manuf. Technol.*

[2] D. F. Williams, L. A. Hayden, and R. B. Marks, “A complete multimode equivalent-circuit theory for electrical design,” to be published in *J. Res. Natl. Inst. Stand. Technol.*

[3] N. Faché and D. De Zutter, “New high-frequency circuit model for coupled lossless and lossy waveguide structures,” *IEEE Trans. Microwave Theory Tech.*, pp. 252-259, March 1990.

[4] P.T. Boggs, R. H. Byrd, and R. D. Schnabel, “A stable and efficient algorithm for nonlinear orthogonal distance regression,” *SIAM J. Sci. and Stat. Comp.*, pp. 1052-1078, Nov. 1987.

[5] W. Heinrich, "Full-wave analysis of conductor losses on MMIC transmission lines," *IEEE Trans. Microwave Theory Tech.*, pp. 1468-1472, Oct. 1990.

[6] R. E. Collin, *Field Theory of Guided Waves*. New York: McGraw-Hill, 1960.

[7] G. Goubau, "On the excitation of surface waves," *Proc. I.R.E.*, pp. 865-868, July 1952.

[8] R. B. Marks and D. F. Williams, "A general waveguide circuit theory," *J. Res. Natl. Inst. Stand. Technol.*, pp. 533-561, Sept.-Oct. 1992.

[9] J. R. Brews, "Transmission line models for lossy waveguide interconnections in VLSI," *IEEE Trans. Electron Dev.*, pp. 1356-1365, 1986.

[10] D. K. Walker, D. F. Williams, and J. M. Morgan, "Planar resistors for probe station calibration," *40th ARFTG Conference Digest*, pp. 68-81, Dec. 1991.

[11] D. F. Williams and F. Olyslager, "Modal cross power in quasi-TEM transmission lines," to be published in *IEEE Microwave Guided Wave Lett.*

[12] F. Olyslager, D. De Zutter, and A. T. de Hoop, "New reciprocal circuit model for lossy waveguide structures based on the orthogonality of the eigenmodes," *IEEE Trans. Microwave Theory Tech.*, pp. 2261-2269, Dec. 1994.